Generation of hybrid Greenberger-Horne-Zeilinger entangled states of particlelike and wavelike optical qubits in circuit QED

Yu Zhang,[1] Tong Liu,[2] Junlong Zhao,[2] Yang Yu,[1] and Chui-Ping Yang[2,3,*]

[1]*School of Physics, Nanjing University, Nanjing 210093, China*

[2]*Quantum Information Research Center, Shangrao Normal University, Shangrao, Jiangxi 334001, China*

[3]*Department of Physics, Hangzhou Normal University, Hangzhou, Zhejiang 311121, China*

(Received 26 March 2020; accepted 4 June 2020; published 26 June 2020)

Hybrid entanglement between particlelike and wavelike optical qubits has drawn increasing attention because such hybrid entanglement is a key resource in establishing hybrid quantum networks and connecting quantum processors with different encoding qubits. For convenience, we define "particlelike optical qubits" as PO qubits and "wavelike optical qubits" as WO qubits. In this work, we propose a method to create a hybrid Greenberger-Horne-Zeilinger (GHZ) entangled state of n PO qubits and n WO qubits, by using $2n$ microwave cavities coupled to a superconducting flux qutrit. The two logic states of a PO qubit here are represented by the vacuum state and the single-photon state of a cavity (or represented by the rotated states of the vacuum state and the single-photon state), while the two logic states of a WO qubit are indicated by the two coherent states of a cavity. The procedure for preparing the GHZ state consists of only a few basic operations, and the circuit resources are significantly reduced because of using only one flux qutrit as the coupler. The GHZ-state preparation time does not depend on the number of qubits, and the GHZ state is deterministically generated since no measurement is made. In addition, the intermediate higher-energy level of the qutrit during the entire operation is virtually excited and thus decoherence from this level is greatly suppressed. This proposal is quite general and can be extended to create the proposed hybrid GHZ state, by using a Λ-type natural or artificial atom coupled to $2n$ microwave or optical cavities. As an example, our numerical simulation demonstrates that within current circuit-QED technology, the hybrid GHZ state of two PO qubits and two WO qubits can be prepared with a high fidelity.

DOI: 10.1103/PhysRevA.101.062334

I. INTRODUCTION AND MOTIVATION

Hybrid entangled states play a crucial role in quantum information processing and quantum technology. For instance, they are helpful in answering fundamental questions, e.g., the border between quantum and classical domains, and the so-called Schrödinger's cat paradox [1], where both microscopic quantum system and macroscopic classical system are entangled with each other. Moreover, hybrid entangled states can act as important quantum channels and intermediate resources for quantum technologies, which cover quantum information transfer, manipulation, and storage between different formats and encodings [2–4]. The subsystems involved in the hybrid entangled states are different in their nature (e.g., an electromagnetic field and a matter system), their size (e.g., microscopic and macroscopic), or in the degree of freedom (e.g., discrete-variable degree and continuous-variable degree). Over the past decades, many schemes have been presented for creating hybrid entangled states in various physical systems, such as trapped ions [5,6], quantum dots [7], cavity QED [8–13], an ensemble of spin-1/2 particles [14], one-dimensional quantum walk [15], and linear optical systems [16–18]. Experimentally, hybrid entangled states have been prepared using (i) polarization of one photon and orbital angular momentum of a second photon [19–22], (ii) polarization of one photon and transverse spatial degree of freedom of the other photon [23], (iii) polarization and orbit angular momentum of a single photon [22,24,25], and (iv) polarization and spatial degree of freedom of a single photon [26,27].

Recently, there is much interest in hybrid entanglement between particlelike optical qubits (PO qubits) and wavelike optical qubits (WO qubits) or between quantum and classical states of light. Hybrid entanglement of light is a key resource in the establishment of hybrid quantum networks and the connection of quantum processors with different encoding qubits. Theoretical proposals have been presented for generating hybrid entangled states of PO qubits and WO qubits in cavity QED or linear optical devices [8,9,11,16–18]. Moreover, hybrid entangled Bell states of a PO qubit and a WO qubit have been experimentally created in a linear optical system [27,28]. After a deep search of literature, we find that the previous works are limited to (i) generation of hybrid entangled states of one PO qubit and one WO qubit [8,9,11,16–18] and (ii) preparation of hybrid entangled states of two PO qubits and one WO qubit via the linear optical devices [16]. However, based on cavity QED or circuit QED, how to create the hybrid entangled Greenberger-Horne-Zeilinger (GHZ) states of n PO qubits and m WO qubits (with $n, m \geqslant 2$) has not been reported yet. As is well known, the GHZ entangled states are of great interest to the foundations of quantum mechanics

*yangcp@hznu.edu.cn

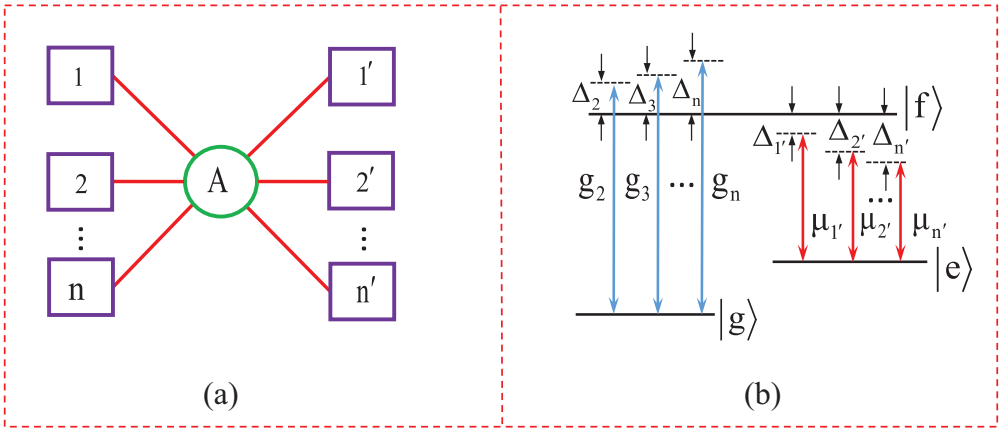

FIG. 1. (a) Schematic circuit of $2n$ microwave cavities coupled to a superconducting flux qutrit (the circle A in the middle). (b) Illustration of $n-1$ cavities $(2, 3, \ldots, n)$ dispersively coupled to the $|g\rangle \leftrightarrow |f\rangle$ transition of the qutrit, while n cavities $(1', 2', \cdots, n')$ dispersively coupled to the $|e\rangle \leftrightarrow |f\rangle$ transition of the qutrit.

and measurement theory. The hybrid GHZ states considered in this work are an important resource for hybrid quantum information processing and hybrid quantum communication (e.g., cryptography and teleportation) with PO qubits and WO qubits. Moreover, they are important in establishing hybrid quantum networks based on PO qubits and WO qubits, and connecting PO-qubit-based quantum processors with WO-qubit-based quantum processors.

The circuit QED, consisting of microwave cavities and artificial atoms, has developed fast in the past decade and has been considered as one of the leading candidates for quantum information processing [29–37]. In the following, we will present an approach to generate a hybrid GHZ entangled state of n PO qubits and n WO qubits, by employing a circuit QED system, which consists of $2n$ microwave cavities coupled to a superconducting flux qutrit. Here, the two logic states of a PO qubit are represented by the vacuum state $|0\rangle$ and the single-photon state $|1\rangle$ of a cavity, or represented by the two rotated basis states $|\pm\rangle = (|0\rangle \pm |1\rangle)/\sqrt{2}$, while the two logic states of a WO qubit are represented by the two coherent states $|\pm\alpha\rangle$ of a cavity. As is well known, coherent states can be considered as a macroscopic state of light, described in a continuous-variable framework. In contrast, a single photon carries the minimum and quantized amount of light energy and thus represents the best example of a microscopic optical quantum system, which is usually described in a discrete-variable framework.

As shown below, our proposal has the following features: (i) The hybrid GHZ state can be prepared with only a few basic operations. (ii) Because only one superconducting flux qutrit is used, the circuit resources are minimized. (iii) The GHZ state preparation time is independent of the number of qubits. (iv) The intermediate higher-energy level for the qutrit is not occupied during the entire operation, thus decoherence from this level is greatly suppressed. (v) The GHZ state can be generated in a deterministic way because no measurement is needed. This proposal is universal and can be applied to accomplish the same task, by employing $2n$ microwave or optical cavities coupled through a Λ-type natural or artificial atom. Furthermore, we numerically demonstrate that the high-fidelity generation of a hybrid GHZ state of two PO qubits and two WO qubits is feasible with current circuit-QED technology.

This paper is arranged as follows. In Sec. II, we introduce an effective Hamiltonian used for the hybrid GHZ-state preparation. In Sec. III, we explicitly show how to generate the hybrid GHZ state of n PO qubits and n WO qubits. In Sec. IV, we give a brief discussion on experimental matters. In Sec. V, as an example, we investigate the experimental feasibility for creating the hybrid GHZ state of two PO qubits and two WO qubits, by using a setup of four one-dimensional (1D) microwave cavities coupled to a superconducting flux qutrit. A concluding summary is presented in Sec. VI.

II. EFFECTIVE HAMILTONIAN

Consider n single-mode cavities $(1, 2, \ldots, n)$ and another n single-mode cavities $(1', 2', \ldots, n')$. The $2n$ cavities are connected by a superconducting flux qutrit A [Fig. 1(a)]. The three levels of the coupler qutrit are labeled as $|g\rangle$, $|e\rangle$, and $|f\rangle$ [Fig. 1(b)]. In general, there exists the transition between the two lowest levels $|g\rangle$ and $|e\rangle$, which, however, can be made to be weak by increasing the barrier between the two potential wells. In this sense, during the GHZ-state preparation, the coupling of the $|g\rangle \leftrightarrow |e\rangle$ transition with the $2n$ cavities can be assumed negligible. The coupling and decoupling of the qutrit from the $2n$ cavities can be achieved by adjustment of the qutrit's level spacings. For superconducting devices, their level spacings can be rapidly (within 1–3 ns) adjusted by varying external control parameters [38,39].

Adjust the level spacings of the coupler qutrit such that the qutrit simultaneously interacts with the $(2n-1)$ cavities $(2, 3, \ldots, n, 1', 2', \ldots, n')$ while it is decoupled from cavity 1. Assume that cavity j is dispersively coupled to the $|g\rangle \leftrightarrow |f\rangle$ transition with a coupling constant g_j and a detuning Δ_j $(j = 2, 3, \ldots, n)$, while highly detuned (decoupled) from the $|e\rangle \leftrightarrow |f\rangle$ and $|g\rangle \leftrightarrow |e\rangle$ transitions. In addition, suppose that cavity j' is dispersively coupled to the $|e\rangle \leftrightarrow |f\rangle$ transition with a coupling constant $\mu_{j'}$ and a detuning $\Delta_{j'}$ $(j' = 1', 2', \ldots, n')$, while highly detuned (decoupled) from the $|g\rangle \leftrightarrow |f\rangle$ and $|g\rangle \leftrightarrow |e\rangle$ transitions. Under these conditions, in the interaction picture and after applying the rotating-wave

approximation (RWA), one has

$$H_I = \sum_{j=2}^{n} g_j (e^{i\Delta_j t} a_j |f\rangle\langle g| + \text{H.c.}) + \sum_{j'=1'}^{n'} \mu_{j'} (e^{i\Delta_{j'} t} b_{j'} |f\rangle\langle e| + \text{H.c.}), \quad (1)$$

where the first term corresponds to the subsystem composed of the coupler qutrit and the $(n-1)$ cavities $(2, 3, \ldots, n)$, while the second term corresponds to the subsystem composed of the coupler qutrit and the n cavities $(1', 2', \ldots, n')$; a_j $(b_{j'})$ is the annihilation operator for the mode of cavity j (j'); Δ_j and $\Delta_{j'}$ are the detunings, given by $\Delta_j = \omega_{fg} - \omega_{c_j}$ and $\Delta_{j'} = \omega_{fe} - \omega_{c_{j'}}$ [Fig. 1(b)]. Here, ω_{fg} (ω_{fe}) is the $|g\rangle \leftrightarrow |f\rangle$ $(|e\rangle \leftrightarrow |f\rangle)$ transition frequency of the qutrit, and ω_{c_j} ($\omega_{c_{j'}}$) is the frequency of cavity j (cavity j').

For the dispersive couplings, i.e., $\Delta_j \gg g_j$ and $\Delta_{j'} \gg \mu_{j'}$, there is no energy exchange between the coupler qutrit and the cavities. Under the condition of

$$\frac{|\Delta_j - \Delta_k|}{|\Delta_j^{-1}| + |\Delta_k^{-1}|} \gg g_j g_k, \quad \frac{|\Delta_{j'} - \Delta_{k'}|}{|\Delta_{j'}^{-1}| + |\Delta_{k'}^{-1}|} \gg \mu_{j'}\mu_{k'}, \quad \frac{|\Delta_j - \Delta_{k'}|}{|\Delta_j^{-1}| + |\Delta_{k'}^{-1}|} \gg g_j \mu_{k'} \quad (2)$$

(where $j, k \in \{2, 3, \ldots, n\}$, $j', k' \in \{1', 2', \ldots, n'\}$, $j \neq k$, $j' \neq k'$), the coupler qutrit does not induce the interaction between the cavities $(2, 3, \ldots, n, 1', 2', \ldots, n')$. Hence, under the dispersive couplings, the effective Hamiltonian is given by [40–42]

$$H_{\text{eff}} = -\sum_{j=2}^{n} \frac{g_j^2}{\Delta_j} (|g\rangle\langle g| a_j^+ a_j - |f\rangle\langle f| a_j a_j^+) - \sum_{j'=1'}^{n'} \frac{\mu_{j'}^2}{\Delta_{j'}} (|e\rangle\langle e| b_{j'}^+ b_{j'} - |f\rangle\langle f| b_{j'} b_{j'}^+), \quad (3)$$

where the terms in the first line account for the ac-Stark shifts of the levels $|g\rangle$ and $|e\rangle$ of the qutrit induced by the cavities $(2, 3, \ldots, n)$, while the terms in the second line are the ac-Stark shifts of the levels $|g\rangle$ and $|e\rangle$ of the qutrit induced by the cavities $(1', 2', \ldots, n')$. When the level $|f\rangle$ is not occupied, the Hamiltonian (3) reduces to

$$H_{\text{eff}} = -\sum_{j=2}^{n} \lambda_j |g\rangle\langle g| a_j^+ a_j - \sum_{j'=1'}^{n'} \lambda_{j'} |e\rangle\langle e| b_{j'}^+ b_{j'}, \quad (4)$$

where $\lambda_j = g_j^2/\Delta_j$ and $\lambda_{j'} = \mu_{j'}^2/\Delta_{j'}$. This Hamiltonian (4) will be employed for the generation of the hybrid GHZ state of particlelike and wavelike optical qubits, as shown in the next section.

III. GENERATION OF HYBRID GHZ STATES OF PARTICLELIKE AND WAVELIKE OPTICAL QUBITS

Let us return to the setup illustrated in Fig. 1(a). Initially, the coupler qutrit is in the ground state $|g\rangle$ and decoupled from the cavity system. Each of the n cavities $(1, 2, \ldots, n)$ is in the state $|+\rangle = (|0\rangle + |1\rangle)/\sqrt{2}$, where $|0\rangle$ and $|1\rangle$ are the vacuum state and the single-photon state. Suppose that each of the n cavities $(1', 2', \ldots, n')$ is in a coherent state $|\alpha\rangle$. Thus, the initial state of the whole system is given by

$$\frac{1}{2^{n/2}} (|0\rangle_1 + |1\rangle_1)(|0\rangle_2 + |1\rangle_2) \ldots (|0\rangle_n + |1\rangle_n) |\alpha\rangle_{1'} |\alpha\rangle_{2'} \ldots |\alpha\rangle_{n'} |g\rangle, \quad (5)$$

where subscripts $1, 2, \ldots, n$ represent cavities $1, 2, \ldots, n$ and subscripts $1', 2', \ldots, n'$ represent cavities $1', 2', \ldots, n'$, respectively. The procedure for generating a hybrid GHZ state of particlelike and wavelike optical qubits is listed below.

Step (i). Adjust the level spacings of the coupler qutrit such that cavity 1 is resonant with the $|g\rangle \leftrightarrow |e\rangle$ transition of the coupler qutrit. The Hamiltonian in the interaction picture and after the RWA is given by $H_r = g_r \hat{a}_1 |e\rangle\langle g| +$ H.c., where the subscript 1 represents cavity 1, g_r is the resonant coupling constant of cavity 1 with the $|g\rangle \leftrightarrow |e\rangle$ transition of the qutrit, and $\hat{a}_1$ is the photon annihilation operator of cavity 1. Under this Hamiltonian, one can obtain the state evolution $|1\rangle_1 |g\rangle \to \cos g_r t |1\rangle_1 |g\rangle - i \sin g_r t |0\rangle_1 |e\rangle$, while the state $|0\rangle_1 |g\rangle$ remains unchanged. For an interaction time $t_1 = \pi/(2g_r)$, it is easy to see that the initial state (5) of the whole system becomes

$$\frac{1}{2^{n/2}} |0\rangle_1 (|g\rangle - i|e\rangle)(|0\rangle_2 + |1\rangle_2)(|0\rangle_3 + |1\rangle_3) \cdots (|0\rangle_n + |1\rangle_n) |\alpha\rangle_{1'} |\alpha\rangle_{2'} \cdots |\alpha\rangle_{n'}. \quad (6)$$

After this step of operation, the level spacings of the coupler qutrit should be adjusted such that the qutrit is decoupled from cavity 1.

Step (ii). Adjust the level spacings of the coupler qutrit such that the qutrit is dispersively coupled to the cavities $(2, 3, \ldots, n, 1', 2', \ldots, n')$ [Fig. 1(b)] to achieve an effective Hamiltonian (4), while the qutrit remains decoupled from cavity 1 . One can verify that under the Hamiltonian (4), the state (6) evolves as

$$\frac{1}{2^{n/2}} |0\rangle_1 [|g\rangle(|0\rangle_2 + e^{i\lambda_2 t}|1\rangle_2)(|0\rangle_3 + e^{i\lambda_3 t}|1\rangle_3) \cdots (|0\rangle_n + e^{i\lambda_n t}|1\rangle_n) |\alpha\rangle_{1'} |\alpha\rangle_{2'} \cdots |\alpha\rangle_{n'} - i|e\rangle(|0\rangle_2 + |1\rangle_2)(|0\rangle_3 + |1\rangle_3) \cdots (|0\rangle_n + |1\rangle_n) |e^{i\lambda_{1'} t}\alpha\rangle_{1'} |e^{i\lambda_{2'} t}\alpha\rangle_{2'} \cdots |e^{i\lambda_{n'} t}\alpha\rangle_{n'}]. \quad (7)$$

By setting

$$|\lambda_2| = |\lambda_3| \cdots = |\lambda_n| = \lambda, \quad |\lambda_{1'}| = |\lambda_{2'}| \cdots = |\lambda_{n'}| = \lambda, \quad (8)$$

and for an interaction time $t_2 = \pi/\lambda$, the state (7) becomes

$$\frac{1}{2^{n/2}} |0\rangle_1 [|g\rangle(|0\rangle_2 - |1\rangle_2)(|0\rangle_3 - |1\rangle_3) \cdots (|0\rangle_n - |1\rangle_n) |\alpha\rangle_{1'} |\alpha\rangle_{2'} \cdots |\alpha\rangle_{n'} - i|e\rangle(|0\rangle_2 + |1\rangle_2)(|0\rangle_3 + |1\rangle_3) \cdots (|0\rangle_n + |1\rangle_n) |-\alpha\rangle_{1'} |-\alpha\rangle_{2'} \cdots |-\alpha\rangle_{n'}]. \quad (9)$$

After this step of operation, the level spacings of the qutrit should be adjusted such that the qutrit is decoupled from the $2n$ cavities.

Step (iii). Adjust the level spacings of the coupler qutrit such that cavity 1 is resonant with the $|g\rangle \leftrightarrow |e\rangle$ transition of

the qutrit. The Hamiltonian is the H_r above, which results in the state evolution $|0\rangle_1|e\rangle \to \cos g_r t|0\rangle_1|e\rangle - i\sin g_r t|1\rangle_1|g\rangle$ while the state $|0\rangle_1|g\rangle$ remains unchanged. For an interaction time $t_3 = 3\pi/(2g_r)$, the state (9) changes to

$$\frac{1}{\sqrt{2}}(|0\rangle_1|-\rangle_2|-\rangle_3\cdots|-\rangle_n|\alpha\rangle_{1'}|\alpha\rangle_{2'}\cdots|\alpha\rangle_{n'} + |1\rangle_1|+\rangle_2 \times|+\rangle_3\cdots|+\rangle_n|-\alpha\rangle_{1'}|-\alpha\rangle_{2'}\cdots|-\alpha\rangle_{n'})\otimes|g\rangle, \quad (10)$$

where $|\pm\rangle_j = (|0\rangle_j \pm |1\rangle_j)/\sqrt{2}$ $(j = 2, 3, \ldots, n)$. After this step of operation, one should adjust the level spacings of the coupler qutrit such that it is decoupled from cavity 1.

The result (10) shows that after the above operations, the $2n$ cavities are disentangled with the coupler qutrit, while n PO qubits $(1, 2, \ldots, n)$ and n WO qubits $(1', 2', \ldots, n')$ are prepared in the hybrid GHZ state

$$|\mathrm{GHZ}\rangle = \frac{1}{\sqrt{2}}(|0\rangle_1|-\rangle_2|-\rangle_3\cdots|-\rangle_n|\alpha\rangle_{1'}|\alpha\rangle_{2'}\cdots|\alpha\rangle_{n'} + |1\rangle_1|+\rangle_2|+\rangle_3\cdots|+\rangle_n|-\alpha\rangle_{1'}|-\alpha\rangle_{2'}\cdots|-\alpha\rangle_{n'}), \quad (11)$$

where the two logical states of the PO qubit 1 are represented by the vacuum state and the single-photon state of cavity 1, the two logical states of the PO qubit j are represented by the two rotated basis states $|+\rangle_j$ and $|-\rangle_j$ of cavity j $(j = 2, 3, \ldots, n)$, while the two logical states of the WO qubit j' are represented by the two coherent states $|\alpha\rangle$ and $|-\alpha\rangle$ of cavity j' $(j' = 1', 2', \ldots, n')$. Note that the two states $|+\rangle$ and $|-\rangle$ of cavity j $(j = 2, 3, \ldots, n)$ can be easily converted into $|0\rangle$ and $|1\rangle$ by performing a local operation on cavity j and an auxiliary qubit placed in cavity j [43].

Based on the description given above, the following can be seen:

(i) During the GHZ-state preparation, the intermediate higher energy level $|f\rangle$ of the coupler qutrit is not occupied and thus decoherence from this level is greatly suppressed.

(ii) There is no measurement performed on the state of the qutrit or the cavities. Thus, the GHZ state is generated in a deterministic way.

(iii) The total operation time for the GHZ-state preparation is

$$t_{\mathrm{op}} = \pi/\lambda + 2\pi/g_r + \pi/g_q + \pi/(4\Omega) + 10\tau_d, \quad (12)$$

which is independent of the number of qubits involved in the prepared GHZ state. Here, τ_d is the typical time required for adjusting the level spacings of the coupler qutrit.

(iv) The coupling or decoupling of the coupler qutrit with the cavities is realized by adjusting the qutrit's level spacings. Alternatively, the coupling or decoupling can be obtained by adjusting the frequency of each cavity. For superconducting microwave cavities, the cavity frequencies can be rapidly (within a few nanoseconds) tuned in experiments [44,45].

(v) The condition (8) turns into

$$\frac{g_2^2}{|\Delta_2|} = \frac{g_3^2}{|\Delta_3|} = \cdots = \frac{g_n^2}{|\Delta_n|} = \frac{\mu_{1'}^2}{|\Delta_{1'}|} = \frac{\mu_{2'}^2}{|\Delta_{2'}|} = \frac{\mu_{3'}^2}{|\Delta_{3'}|} = \cdots = \frac{\mu_{n'}^2}{|\Delta_{n'}|}. \quad (13)$$

Because of $\Delta_j = \omega_{fg} - \omega_{c_j}$ and $\Delta_{j'} = \omega_{fe} - \omega_{c_{j'}}$ the equality given in Eq. (13) can be easily established by selecting the Δ_j via adjusting the frequency of cavity j $(j = 2, 3, \ldots, n)$ and selecting the $\Delta_{j'}$ via adjusting the frequency of cavity j' $(j' = 1', 2', \ldots, n')$.

We should mention that the initial state $|+\rangle$ for each of the n cavities $(1, 2, \ldots, n)$ can be easily prepared. To prepare the state $|+\rangle$ for cavity l $(l = 1, 2, \ldots, n)$, one can place qubit l (i.e., a two-level qubit with a ground level $|g\rangle$ and an excited level $|e\rangle$) in cavity l and apply a microwave pulse to qubit l initially in the ground state $|g\rangle_l$. The pulse is resonant with the $|g\rangle \leftrightarrow |e\rangle$ transition of the qubit. After a pulse-qubit interaction time $\pi/(2\Omega_l)$ (Ω_l being the pulse Rabi frequency), the state transformation $|g\rangle_l \to (|g\rangle_l - i|e\rangle_l)/\sqrt{2}$ can be obtained [43]. Then, have cavity l (initially in the vacuum state $|0\rangle_l$) resonant with the $|g\rangle \leftrightarrow |e\rangle$ transition of qubit l for an interaction time $\pi/(2\chi_l)$. Here, χ_l is the cavity-qubit coupling constant. As a result, the state transformation $(|g\rangle_l - i|e\rangle_l)|0\rangle_l/\sqrt{2} \to |g\rangle_l(|0\rangle_l + |1\rangle_l)/\sqrt{2}$ is achieved [43], i.e., cavity l is prepared in the state $|+\rangle_l$. Because only resonant interaction is used, the state $|+\rangle_l$ can be fast prepared within a very short time. In addition, it is noted that the state $|+\rangle$ for each of the n cavities $(1, 2, \ldots, n)$ can be almost simultaneously created because the local operations on the individual cavities and their hosting qubits can be parallelly performed at the same time. Thus, decoherence is negligible during the preparation of the state $|+\rangle$ for the n cavities $(1, 2, \ldots, n)$. Note that the cavity-qubit (or pulse-qubit) coupling and decoupling, involved during the preparation of the state $|+\rangle$, can be achieved by adjusting the qubit-level spacings or the cavity frequency.

Alternatively, it is straightforward to see that the initial state $|+\rangle$ of cavity l $(l = 1, 2, \ldots, n)$ can be prepared through the same state transformations described above, by applying a microwave pulse resonant with the $|g\rangle \leftrightarrow |e\rangle$ transition of the coupler qutrit mentioned previously, and then having cavity l resonant with $|g\rangle \leftrightarrow |e\rangle$ transition of the coupler qutrit. The advantage of this approach is that no auxiliary qubit needs to be placed in each cavity but the operation time for creating the state $|+\rangle$ for all the n cavities $(1, 2, \ldots, n)$ increases with the number of the cavities and thus decoherence will pose a problem. However, it is noted that this alternative method is preferable for a small number of the cavities.

IV. DISCUSSION

It is necessary to give a brief discussion on experimental matters. Several points are made as follows:

(i) Decoherence from the coupler qutrit in the operations of steps (i) and (iii) can be neglected because these operations are performed within a very short time due to using the resonant cavity-qutrit interactions. Hence, the main problem caused by the decoherence lies in the operation of step (ii) above, which requires a quite long operation time π/λ due to using the dispersive cavity-qutrit interaction.

(ii) To make the effect of decoherence from the coupler qutrit negligible, the operation time π/λ of step (ii) should be much smaller than the energy relaxation time T_1 and the dephasing time T_2 of the level $|e\rangle$ as well as the energy relaxation time T_1' and the dephasing time T_2' of the level

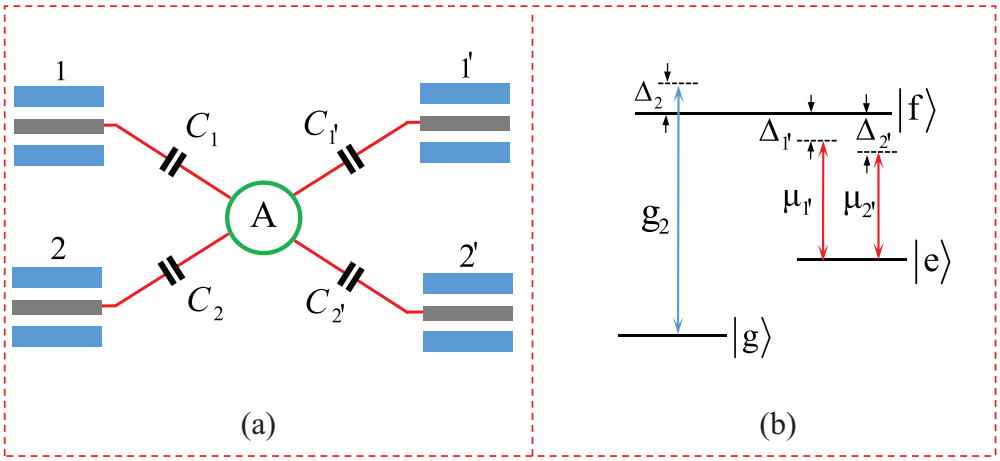

FIG. 2. (a) Schematic circuit of four 1D microwave cavities coupled to a superconducting flux qutrit. (b) Illustration of cavity 2 dispersively coupled with the $|g\rangle \leftrightarrow |f\rangle$ transition of the qutrit, while cavities $1'$ and $2'$ dispersively coupled with the $|e\rangle \leftrightarrow |f\rangle$ transition of the qutrit. The unwanted couplings or interactions of the qutrit's energy-level transitions with the cavities are not illustrated in (b) for simplicity, which, however, are considered in our numerical simulation, as described in the Hamiltonian (15).

$|f\rangle$ of the coupler qutrit. Note that $\pi/\lambda \ll T_1', T_2'$ can be readily met because the level $|f\rangle$ is unpopulated during the entire operation. In addition, $\pi/\lambda \ll T_1, T_2$ can be achieved by choosing the coupler qutrit with sufficiently long T_1 and T_2 of the level $|e\rangle$. Alternatively, these conditions can be met by shortening π/λ. Note that π/λ can be shortened by increasing λ (through an optimal choice of the ratio $|\Delta_j|/g_j, |\Delta_{j'}|/\mu_{j'}$).

(iii) The photon lifetime of cavity k ($k = 1, 2, \ldots, n, 1', 2', \ldots, n'$) is given by $T_{\rm cav}^k = Q_k/(\omega_k \bar{n}_k)$, where Q_k, ω_k, and $\bar{n}_k$ are the quality factor, the frequency, and the average photon number of cavity k, respectively. For the $2n$ cavities here, the minimum photon lifetime is given by [46]

$$T_{\rm cav} = \frac{1}{2n} \min\left\{T_{\rm cav}^1, T_{\rm cav}^2, \ldots, T_{\rm cav}^n, T_{\rm cav}^{1'}, T_{\rm cav}^{2'}, \ldots, T_{\rm cav}^{n'}\right\}, \quad (14)$$

which should be much longer than $t_{\rm op}$, such that the decay of each cavity is negligible during the operation. In principle, this condition can be met by choosing cavities with a high-quality factor.

(iv) When the coupler qutrit is a solid-state qutrit, there may exist an intercavity crosstalk during the GHZ preparation. However, because this proposal employs cavities of different frequencies, the unwanted intercavity crosstalk can be made negligibly small by having the frequency difference between any two cavities be much larger than the coupling strength of the two cavities.

V. POSSIBLE EXPERIMENTAL IMPLEMENTATION

In this section, as an example, we investigate the experimental feasibility for creating the hybrid GHZ state of two PO qubits (1,2) and two WO qubits ($1', 2'$) [i.e., the GHZ state (11) with $n = 2$ and $n' = 2'$], by using a setup of four 1D microwave cavities coupled to a superconducting flux qutrit [Fig. 2(a)]. Let us now give a discussion on the fidelity of the operations. Since only the resonant interactions are used in steps (i) and (iii), these two steps can be completed within a very short time (e.g., by increasing g_r), such that the effect of the qutrit decoherence, the cavity dissipation, and the intercavity crosstalk is negligibly small for the steps (i) and (iii). In this case, the effect of the system dissipation and the intercavity crosstalk would appear in the operation of step (ii) because of using the qutrit-cavity dispersive interaction [Fig. 2(b)].

When the unwanted couplings between the qutrit's level transitions and the cavities as well as the intercavity crosstalk are considered, the Hamiltonian H_I in Eq. (1), with $n = 2$ and $n' = 2'$ for the present case, is modified as (without RWA)

$$\begin{aligned} H_I' = {} & (e^{i\omega_{c_2}t} a_2^+ + \text{H.c.})(g_2 e^{i\omega_{fg}t}|f\rangle\langle g| + g_2' e^{i\omega_{fe}t}|f\rangle\langle e| \\ & + g_2'' e^{i\omega_{eg}t}|e\rangle\langle g| + \text{H.c.}) + (e^{i\omega_{c_{1'}}t} b_{1'}^+ + \text{H.c.})(\mu_{1'}' e^{i\omega_{fg}t}|f\rangle \\ & \times \langle g| + \mu_{1'} e^{i\omega_{fe}t}|f\rangle\langle e| + \mu_{1'}'' e^{i\omega_{eg}t}|e\rangle\langle g| + \text{H.c.}) \\ & + (e^{i\omega_{c_{2'}}t} b_{2'}^+ + \text{H.c.})(\mu_{2'}' e^{i\omega_{fg}t}|f\rangle\langle g| + \mu_{2'} e^{i\omega_{fe}t}|f\rangle\langle e| \\ & + \mu_{2'}'' e^{i\omega_{eg}t}|e\rangle\langle g| + \text{H.c.}) + \varepsilon, \end{aligned} \quad (15)$$

where g_2' (g_2'') is the coupling constant between cavity 2 and the $|e\rangle \to |f\rangle$ ($|g\rangle \to |e\rangle$) transition, $\mu_{1'}'$ ($\mu_{1'}''$) is the coupling constant between cavity $1'$ and the $|g\rangle \to |f\rangle$ ($|g\rangle \to |e\rangle$) transition, $\mu_{2'}'$ ($\mu_{2'}''$) is the coupling constant between cavity $2'$ and the $|g\rangle \to |f\rangle$ ($|g\rangle \to |e\rangle$) transition, ω_{eg} is the $|g\rangle \leftrightarrow |e\rangle$ transition frequency of the qutrit, and ω_{c_l} is the frequency of cavity l ($l = 2, 1', 2'$). In addition, ε is the Hamiltonian describing the intercavity crosstalk, given by

$$\begin{aligned} \varepsilon = {} & (g_{12} e^{i\Delta_{12}t} a_1^+ a_2 + \text{H.c.}) + (g_{1'2'} e^{i\Delta_{1'2'}t} b_{1'}^+ b_{2'} + \text{H.c.}) \\ & + (g_{11'} e^{i\Delta_{11'}t} a_1^+ b_{1'} + \text{H.c.}) + (g_{12'} e^{i\Delta_{12'}t} a_1^+ b_{2'} + \text{H.c.}) \\ & + (g_{21'} e^{i\Delta_{21'}t} a_2^+ b_{1'} + \text{H.c.}) + (g_{22'} e^{i\Delta_{22'}t} a_2^+ b_{2'} + \text{H.c.}), \end{aligned} \quad (16)$$

where g_{kl} is the crosstalk strength between the two cavities k and l with the frequency difference $\Delta_{kl} = \omega_{c_k} - \omega_{c_l}$ ($k, l \in \{1, 2, 1', 2'\}; k \neq l$).

During the operation of step (ii), the dynamics of the lossy system is determined by

$$\frac{d\rho}{dt} = -i[H_I', \rho] + \sum_{j=1}^{2} \kappa_j \mathcal{L}[a_j] + \sum_{j'=1'}^{2'} \kappa_{j'} \mathcal{L}[b_{j'}] + \gamma_{eg}\mathcal{L}[\sigma_{eg}^-] + \gamma_{fe}\mathcal{L}[\sigma_{fe}^-] + \gamma_{fg}\mathcal{L}[\sigma_{fg}^-] + \gamma_{e,\varphi}(\sigma_{ee}\rho\sigma_{ee} - \sigma_{ee}\rho/2 - \rho\sigma_{ee}/2) + \gamma_{f,\varphi}(\sigma_{ff}\rho\sigma_{ff} - \sigma_{ff}\rho/2 - \rho\sigma_{ff}/2), \quad (17)$$

where $\mathcal{L}[\Lambda] = \Lambda\rho\Lambda^+ - \Lambda^+\Lambda\rho/2 - \rho\Lambda^+\Lambda/2$ (with $\Lambda = a_j, , b_{j'}, \sigma_{eg}^-, \sigma_{fe}^-, \sigma_{fg}^-$), $\sigma_{eg}^- = |g\rangle\langle e|$, $\sigma_{fe}^- = |e\rangle\langle f|$, $\sigma_{fg}^- = |g\rangle\langle f|$, $\sigma_{ee} = |e\rangle\langle e|$, and $\sigma_{ff} = |f\rangle\langle f|$. In addition, κ_j ($\kappa_{j'}$) is the decay rate of cavity j (j'); γ_{eg} is the energy relaxation rate for the level $|e\rangle$ of the qutrit associated with the decay path $|e\rangle \to |g\rangle$; γ_{fe} (γ_{fg}) is the relaxation rate for the level $|f\rangle$ of the qutrit related to the decay path $|f\rangle \to |e\rangle$ ($|f\rangle \to |g\rangle$); and $\gamma_{e,\varphi}$ ($\gamma_{f,\varphi}$) is the dephasing rate of the level $|e\rangle$ ($|f\rangle$) of the qutrit.

The fidelity of the entire operation is given by $\mathcal{F} = \sqrt{\langle\psi_{id}|\rho|\psi_{id}\rangle}$, where $|\psi_{id}\rangle$ is the ideal output state given by Eq. (10) for $n = 2$ and $n' = 2'$, while ρ is the final density matrix obtained by numerically solving the master equation.

For a flux qutrit, the typical transition frequency between neighboring levels can be made as 1–20 GHz. As an example, consider $\omega_{eg}/2\pi = 2.0\,\text{GHz}$, $\omega_{fe}/2\pi = 4.5\,\text{GHz}$, and $\omega_{fg}/2\pi = 6.5\,\text{GHz}$. Assume $\omega_{c_1}/2\pi = 1.5\,\text{GHz}$ for cavity 1. With a choice of $\Delta_2/2\pi = -1.5\,\text{GHz}$, $\Delta_{1'}/2\pi = 1.0\,\text{GHz}$, and $\Delta_{2'}/2\pi = 1.5\,\text{GHz}$, we have $\omega_{c_2}/2\pi = 8.0\,\text{GHz}$, $\omega_{c_{1'}}/2\pi = 3.5\,\text{GHz}$, and $\omega_{c_{2'}}/2\pi = 3.0\,\text{GHz}$. Thus, we have $\Delta_{12}/2\pi = -6.5\,\text{GHz}$, $\Delta_{1'2'}/2\pi = 0.5\,\text{GHz}$, $\Delta_{11'}/2\pi = -2.0\,\text{GHz}$, $\Delta_{12'}/2\pi = -1.5\,\text{GHz}$, $\Delta_{21'}/2\pi = 4.5\,\text{GHz}$, and $\Delta_{22'}/2\pi = 5.0\,\text{GHz}$. For the values of Δ_2, $\Delta_{1'}$, and $\Delta_{2'}$ here and by choosing $g_2/2\pi = 50\,\text{MHz}$, we have $\mu_{1'}/2\pi \simeq 40.8\,\text{MHz}$ and $\mu_{2'}/2\pi = 50\,\text{MHz}$ according to Eq. (13). The coupling constants here are readily available because a coupling constant $\sim 2\pi \times 230\,\text{MHz}$ was reported for a flux device coupled to a one-dimensional coplanar waveguide resonator or cavity [47].

Note that the dipole matrix element between the two levels $|g\rangle$ and $|f\rangle$ can be made to be on the same order as that between the two levels $|e\rangle$ and $|f\rangle$ with appropriate design of the qutrit system [48]; while the matrix element between the two levels $|g\rangle$ and $|e\rangle$ can be made much weaker by increasing the potential barrier of the qutrit, as mentioned previously. Thus, we choose $g_2' \sim g_2$, $g_2'' \sim 0.1g_2$; $\mu_{1'}' \sim \mu_{1'}$, $\mu_{1'}'' \sim 0.1\mu_{1'}$; and $\mu_{2'}' \sim \mu_{2'}$, $\mu_{2'}'' \sim 0.1\mu_{2'}$. Additional parameters used in the numerical simulation are as follows: (i) $\gamma_{eg}^{-1} = 5T\ \mu\text{s}$, $\gamma_{fe}^{-1} = 2T\ \mu\text{s}$, $\gamma_{fg}^{-1} = T\ \mu\text{s}$; (ii) $\gamma_{\phi e}^{-1} = \gamma_{\phi f}^{-1} = T\ \mu\text{s}$; (iii) $\kappa_1, \kappa_2, \kappa_{1'}, \kappa_{2'} = \kappa$; and (v) $\alpha = 2$. In addition, choose $g_{kl} = 0.01g_m$ with $g_m = \max\{g_2, g_2', g_2'', \mu_{1'}, \mu_{1'}', \mu_{1'}'', \mu_{2'}, \mu_{2'}', \mu_{2'}''\}$, which is achievable in experiments by a prior design of the sample with appropriate capacitances $c_1, c_2, c_{1'}, c_{2'}$ [46].

By solving the master equation (17), we numerically plot Fig. 3, which illustrates the fidelity versus T and κ^{-1}. From Fig. 3, one can see that when $T \geqslant 5\ \mu\text{s}$ and $\kappa^{-1} \geqslant 10\ \mu\text{s}$, the fidelity exceeds 96.9%, which implies that the high-fidelity generation of the hybrid GHZ state of two PO qubits and two WO qubits can be obtained for the GHZ state prepared in a realistic situation. We remark that when the qutrit decoherence, the cavity decay, and the intercavity crosstalk are considered in the operations of steps (i) and (iii), the fidelity would be slightly decreased but will not be decreased greatly because these two steps of operation can be completed very fast due to the use of the resonant interactions.

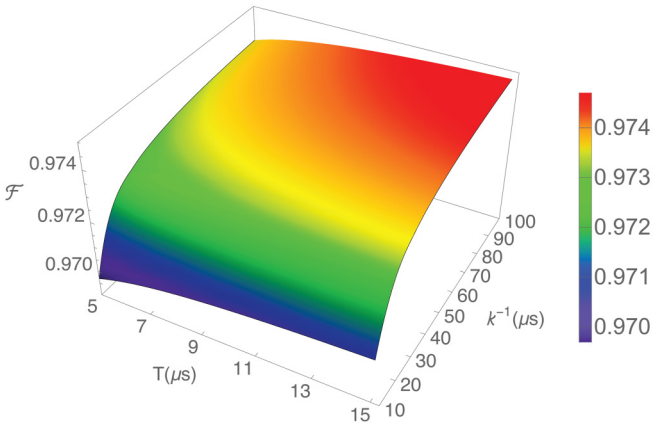

FIG. 3. Fidelity versus T and κ^{-1}. The parameters used in the numerical simulation are referred to in the text.

As shown above, a flux qutrit is used as a Λ-type artificial atom. For a flux qutrit, the Λ-type level structure, formed by the lowest three levels, can be obtained by having the external magnetic flux away from the degenerate point $f = 0.5$ [48]. However, it is noted that the influence of flux noise would be greatly increased with the increment of the deviation from $f = 0.5$. Thus, the deviation value from the degenerate point $f = 0.5$ needs to be carefully selected in order to reduce the effect of the flux noise on the operational fidelity.

With the parameters chosen above, the GHZ state production time is estimated as $\sim$0.32 μs, much shorter than the decoherence times of the qutrit (5–75 μs) and the cavity decay times (10–100 μs) considered in Fig. 3. In our numerical simulation, we consider a rather conservative case for decoherence time of the flux qutrit, because experiments have reported decoherence time 70 μs to 1 ms for a superconducting flux device [49,50]. During the GHZ state preparation, the average photon numbers are estimated as $\bar{n}_1 = \bar{n}_2 = 0.5$ for cavities (1,2), while $\bar{n}_{1'} = \bar{n}_{2'} = 4$ for cavities ($1', 2'$) due to the $\alpha = 2$ used in the numerical simulation. Thus, for $\kappa^{-1} = 10\ \mu\text{s}$ and the cavity frequencies given above, a simple calculation gives $Q_1 \sim 4.71 \times 10^4$ for cavity 1, $Q_2 \sim 2.51 \times 10^5$ for cavity 2, $Q_{1'} \sim 8.79 \times 10^5$ for cavity $1'$, and $Q_{2'} \sim 7.53 \times 10^5$ for cavity $2'$. Note that a high-quality factor $Q \sim 10^6$ of a 1D microwave cavity or resonator has been experimentally demonstrated [51,52]. Our analysis here implies that the high-fidelity generation of the hybrid GHZ state of two PO qubits and two WO qubits is feasible within the current circuit QED technology.

VI. CONCLUSION

We have presented an approach to generate the hybrid GHZ state of n particlelike optical qubits and n wavelike optical qubits, by employing a circuit-QED system. This proposal has the following features: (i) Because only a few basic

operations are needed for the hybrid GHZ state preparation, this proposal is simple to implement in experiments. (ii) Only one superconducting flux qutrit is used as a coupler; the circuit architecture is greatly simplified. (iii) The entire operation time required for the GHZ-state preparation is independent of the number of qubits, and thus does not increase when increasing the number of qubits. (iv) The intermediate higher-energy level $|f\rangle$ of the coupler qutrit is not occupied during the entire operation, thus the decoherence from this level is greatly suppressed. (v) The GHZ state is generated deterministically because no measurement is required. This proposal is universal and can be applied to accomplish the same task by employing $2n$ optical or microwave cavities coupled to a Λ-type natural or artificial atom. Finally, numerical simulations demonstrate that the high-fidelity generation of a hybrid GHZ state of two particlelike optical qubits and two wavelike optical qubits is feasible with current circuit-QED technology.

ACKNOWLEDGMENTS

This work was partly supported by the Key-Area Research and Development Program of Guangdong Province (Grant No. 2018B030326001), the National Natural Science Foundation of China (NSFC) (Grants No. 11074062, No. 11374083, No. 11774076, No. 11890704, and No. 61521001), the Jiangxi Natural Science Foundation (Grant No. 20192ACBL20051), and the NKRDP of China (Grant No. 2016YFA0301802).

[1] E. Schrödinger, Die gegenwaertige situation in der quantenmechanik, Naturwissenschaften **23**, 823 (1935).

[2] M. Silva and C. R. Myers, Computation with coherent states via teleportations to and from a quantum bus, Phys. Rev. A **78**, 062314 (2008).

[3] L. P. van, Optical hybrid approaches to quantum information, Laser Photonics Rev. **5**, 167 (2011).

[4] U. L. Andersen, J. S. Neergaard-Nielsen, L. P. van, and A. Furusawa, Hybrid quantum information processing, Nat. Phys. **11**, 713 (2015).

[5] J. Q. Liao, Y. Guo, H. S. Zeng, and L. M. Kuang, Preparation of hybrid entangled states and entangled coherent states for a single trapped ion in a cavity, J. Phys. B: At., Mol. Opt. Phys. **39**, 4709 (2006).

[6] N. Mohseni, S. Saeidian, J. P. Dowling, and C. Navarrete-Benlloch, Deterministic generation of hybrid high-N00N states with Rydberg ions trapped in microwave cavities, Phys. Rev. A **101**, 013804 (2020).

[7] F. Domínguez-Serna and F. Rojas, Spin-orbit hybrid entangled channel for spin state quantum teleportation using genetic algorithms, Quantum Inf. Process. **18**, 32 (2019).

[8] S. B. Zheng, Preparation of even and odd coherent states in the motion of a cavity mirror, Quantum Semiclassical Opt. **10**, 657 (1998).

[9] C. P. Yang, Q. P. Su, S. B. Zheng, F. Nori, and S. Han, Entangling two oscillators with arbitrary asymmetric initial states, Phys. Rev. A **95**, 052341 (2017).

[10] Y. S. Zhou, X. Li, Y. Deng, H. R. Li, and M. X. Luo, Generation of hybrid four-qubit entangled decoherence-free states assisted by the cavity-QED system, Opt.Commun. **366**, 397 (2016).

[11] Z. B. Chen, G. Hou, and Y. D. Zhang, Quantum nonlocality and applications in quantum-information processing of hybrid entangled states, Phys. Rev. A **65**, 032317 (2002).

[12] Z. T. Yang, C. Cao, and C. Wang, Generation of entangled and hyperentangled bell states on photon systems assisted by diamond nitrogen-vacancy centers coupled with whispering-gallery-mode microresonators, Int. J. Theor. Phys. **58**, 2200 (2019).

[13] J. Joo and E. Ginossar, Efficient scheme for hybrid teleportation via entangled coherent states in circuit quantum electrodynamics, Sci. Rep. **6**, 26338 (2016).

[14] T. Pramanik, S. Adhikari, A. S. Majumdar, D. Home, and A. K. Pan, Information transfer using a single particle path-spin hybrid entangled state, Phys. Lett. A **374**, 1121 (2010).

[15] A. Gratsea, M. Lewenstein, and A. Dauphin, Generation of hybrid maximally entangled states in a one-dimensional quantum walk, Quantum Sci. Technol. **5**, 025002 (2020).

[16] S. A. Podoshvedov, Mechanism of interaction of discrete and continuous variable states for efficient generation of hybrid entangled states, arXiv:1805.07519.

[17] S. H. Xiang and K. H. Song, Non-Gaussian correlation estimates of two-mode hybrid entangled states via cross-Kerr medium and cumulant method, Eur. Phys. J. D **72**, 185 (2018).

[18] Y. Li, H. Jing, and M. S. Zhan, Optical generation of a hybrid entangled state via an entangling single-photon-added coherent state, J. Phys. B: At., Mol. Opt. Phys. **39**, 2107 (2006).

[19] E. Nagali and F. Sciarrino, Generation of hybrid polarization-orbital angular momentum entangled states, Opt. Express **18**, 18243 (2010).

[20] R. Fickler, G. Campbell, B. Buchler, P. K. Lam, and A. Zeilinger, Quantum entanglement of angular momentum states with quantum numbers up to 10,010, Proc. Natl. Acad. Sci. USA **113**, 13642 (2016).

[21] M. V. Jabir, N. A. Chaitanya, M. Mathew, and G. K. Samanta, Direct transfer of classical nonseparable states into hybrid entangled two photon states, Sci. Rep. **7**, 7331 (2017).

[22] E. Karimi, J. Leach, S. Slussarenko, B. Piccirillo, L. Marrucci, L. Chen, W. She, S. Franke-Arnold, M. J. Padgett, and E. Santamato, Spin-orbit hybrid entanglement of photons and quantum contextuality, Phys. Rev. A **82**, 022115 (2010).

[23] W. A. T. Nogueira, M. Santibañez, S. Pádua, A. Delgado, C. Saavedra, L. Neves, and G. Lima, Interference and complementarity for two-photon hybrid entangled states, Phy. Rev. A **82**, 042104 (2010).

[24] J. T. Barreiro, T. C. Wei, and P. G. Kwiat, Remote Preparation of Single-Photon "Hybrid" Entangled and Vector-Polarization States, Phy. Rev. Lett. **105**, 030407 (2010).

[25] J. T. Barreiro, T. C. Wei, and P. G. Kwiat, Beating the channel capacity limit for linear photonic superdense coding, Nat. Phys. **4**, 282 (2008).

[26] D. Boschi, S. Branca, F. D. Martini, L. Hardy, and S. Popescu, Experimental Realization of Teleporting an Unknown Pure Quantum State via Dual Classical and Einstein-Podolsky-Rosen Channels, Phys. Rev. Lett. **80**, 1121 (1998).

[27] M. Michler, H. Weinfurter, and M. Zukowski, Experiments towards Falsification of Noncontextual Hidden Variable Theories, Phys. Rev. Lett. **84**, 5457 (2000).

[28] O. Morin, K. Huang, J. Liu, H. L. Jeannic, C. Fabre, and J. Laurat, Remote creation of hybrid entanglement between partical-like and wave-like optical qubits, Nat. Photonics **8**, 570 (2014).

[29] C. P. Yang, S. I. Chu, and S. Han, Possible realization of entanglement, logical gates, and quantum information transfer with superconducting-quantuminterference-device qubits in cavity QED, Phys. Rev. A **67**, 042311 (2003).

[30] J. Q. You and F. Nori, Quantum information processing with superconducting qubits in a microwave field, Phys. Rev. B **68**, 064509 (2003).

[31] A. Blais, R. S. Huang, A. Wallra, S. M. Girvin, and R. J. Schoelkopf, Cavity quantum electrodynamics for superconducting electrical circuits: An architecture for quantum computation, Phys. Rev. A **69**, 062320 (2004).

[32] J. Q. You and F. Nori, Superconducting circuits and quantum information, Phys. Today **58**(11), 42 (2005).

[33] J. Clarke and F. K. Wilhelm, Superconducting quantum bits, Nature (London) **453**, 1031 (2008).

[34] J. Q. You and F. Nori, Atomic physics and quantum optics using superconducting circuits, Nature (London) **474**, 589 (2011).

[35] Z. L. Xiang, S. Ashhab, J. Q. You, and F. Nori, Hybrid quantum circuits: Superconducting circuits interacting with other quantum systems, Rev. Mod. Phys. **85**, 623 (2013).

[36] X. Gu, A. F. Kockum, A. Miranowicz, Y. X. Liu, and F. Nori, Microwave photonics with superconducting quantum circuits, Phys. Rep. **718**, 1 (2017).

[37] P. B. Li, Y. C. Liu, S. Y. Gao, Z. L. Xiang, P. Rabl, Y.F. Xiao, and F. L. Li, Hybrid Quantum Device Based on NV Centers in Diamond Nanomechanical Resonators Plus Superconducting Waveguide Cavities, Phys. Rev. Appl. **4**, 044003 (2015).

[38] P. J. Leek, S. Filipp, P. Maurer, M. Baur, R. Bianchetti, J. M. Fink, M. Goppl, L. Steffen, and A. Wallraff, Using sideband transitions for two-qubit operations in superconducting circuits, Phys. Rev. B **79**, 180511 (2009).

[39] M. Neeley, M. Ansmann, R. C. Bialczak, M. Hofheinz, N. Katz, E. Lucero, A. O'Connell, H. Wang, A. N. Cleland, and J. M. Martinis, Process tomography of quantum memory in a Josephson-phase qubit coupled to a two-level state, Nat. Phys. **4**, 523 (2008).

[40] S. B. Zheng and G. C. Guo, Efficient Scheme for Two-Atom Entanglement and Quantum Information Processing in Cavity QED, Phys. Rev. Lett. **85**, 2392 (2000).

[41] A. Sørensen and K. Mølmer, Quantum Computation with Ions in Thermal Motion, Phys. Rev. Lett. **82**, 1971 (1999).

[42] D. F. V. James and J. Jerke, Effective Hamiltonian theory and its applications in quantum information, Can. J. Phys. **85**, 625 (2007).

[43] C. P. Yang and S. Han, *n*-qubit-controlled phase gate with superconducting quantum-interference devices coupled to a resonator, Phys. Rev. A **72**, 032311 (2005).

[44] M. Sandberg, C. M. Wilson, F. Persson, T. Bauch, G. Johansson, V. Shumeiko, T. Duty, and P. Delsing, Tuning the field in a microwave resonator faster than the photon lifetime, Appl. Phys. Lett. **92**, 203501 (2008).

[45] Z. L. Wang, Y. P. Zhong, L. J. He, H. Wang, J. M. Martinis, A. N. Cleland, and Q. W. Xie, Quantum state characterization of a fast tunable superconducting resonator, Appl. Phys. Lett. **102**, 163503 (2013).

[46] C. P. Yang, Q. P. Su, and S. Han, Generation of Greenberger-Horne-Zeilinger entangled states of photons in multiple cavities via a superconducting qutrit or an atom through resonant interaction, Phys. Rev. A **86**, 022329 (2012).

[47] K. Inomata, T. Yamamoto, P.-M. Billangeon, Y. Nakamura, and J. S. Tsai, Large dispersive shift of cavity resonance induced by a superconducting flux qubit in the straddling regime, Phys. Rev. B **86**, 140508(R) (2012).

[48] Y. X. Liu, J. Q. You, L. F. Wei, C. P. Sun, and F. Nori, Optical Selection Rules and Phase-Dependent Adiabatic State Control in a Superconducting Quantum Circuit, Phys. Rev. Lett. **95**, 087001 (2005).

[49] F. Yan, S. Gustavsson, A. Kamal, J. Birenbaum, A. P. Sears, D. Hover, T. J. Gudmundsen, J. L. Yoder, T. P. Orlando, J. Clarke, A. J. Kerman, and W. D. Oliver, The flux qubit revisited to enhance coherence and reproducibility, Nat. Commun. **7**, 12964 (2016).

[50] J. Q. You, X. Hu, S. Ashhab, and F. Nori, Low-decoherence flux qubit, Phys. Rev. B **75**, 140515(R) (2007).

[51] W. Chen, D. A. Bennett, V. Patel, and J. E. Lukens, Substrate and process dependent losses in superconducting thin film resonators, Supercond. Sci. Technol. **21**, 075013 (2008).

[52] P. J. Leek, M. Baur, J. M. Fink, R. Bianchetti, L. Steffen, S. Filipp, and A. Wallraff, Cavity Quantum Electrodynamics with Separate Photon Storage and Qubit Readout Modes, Phys. Rev. Lett. **104**, 100504 (2010).